Dynamic Constitutive Equation Considering Temperature Rise for Polyester Filament Yarns

DYNAMIC CONSTITUTIVE EQUATION CONSIDERING TEMPERATURE RISE FOR POLYESTER FILAMENT YARNS

By Toshiyasu KINARI*, Akihiro HOJO*, Sukenori SHINTAKU**
Nobuo IWAKI** and Yoshiyuki HARASHINO***

Key words; Polyester filament yarn, Constitutive equation, Stress-strain curve, Temperature rise, Dynamic mechanical properties

1. INTRODUCTION

According to speed up of textile machinery, yarn velocity has become larger on the textile process. And textile yarns are often subjected to impact load. So it is important to clarify their dynamic mechanical properties. The authors have investigated the dynamic mechanical properties of polyester multi-filament yarn using a new impact tensile testing apparatus and introducing the over-stress theory [1] to express their stress-strain curves [2]. The over-stress theory well explained stress-strain curves at low strain rates (less than 10^{-2} s^{-1}), but the calculated stress became larger than the experimental data with increasing strain and strain rate at high strain rates. This seemed to be influenced by softening with temperature rise in filaments during extension because the deformation proceeded too rapidly to disperse the generated heat. There were many reports related to heat generated in yarn at impact tensile tests [3 - 5]. Hall [6] calculated temperature rise in fiber at tensile test by considering thermodynamics. So we introduced this effect into the constitutive equation [7] by means of estimating the temperature rise during extension at high strain rates and compared the calculated stress-strain curves with the experimental ones. But in our past papers [2, 7], the only one kind of yarn is investigated. The present report is concerned with the expansion of data regarding this object and the presentation of results. Six kinds of polyester filament yarn specimens which differ in drawing temperature or in spinning speed are tested at strain rates ranging from the order of 10^{-3} to 10^{2} s^{-1} and the resultant stress-strain curves are compared with the theoretical ones.

* *Faculty of Technology, Kanazawa University ; Member of the Society of Material Science, Japan, and of the Japan Society of Mechanical Engineers.*
** *Faculty of Technology, Kanazawa University ;Member of the Japan Society of Mechanical Engineers, and of the Society of Fiber Science and Technology, Japan.*
*** *Graduate Student of Kanazawa University; Student Member of the Society of Fiber Science and Technology, Japan.*

2. EXPERIMENTAL METHOD

Figure 1 shows the schematic diagram of the experimental apparatus. It is mainly composed of the cantilever type load cell, the input bar and base. The yarn specimen is bonded to a couple of aluminium chips at both ends with epoxy resin. It is placed between the load cell and input bar through each slit, and is elongated by pushing down the input bar. The mass of the input bar being 48 g, the specimen is to be pre-tensioned of 0.47 N that is not very small compared with the load of investigated yarns. Therefore, the stress-strain curves less than 0.47 N in load are extrapolated. The load is measured by means of the semi-conductor gauge (KYOWA ELECTRONIC INSTRUMENTS KSP-1-350-E4) bonded near the fixed end of the load cell.

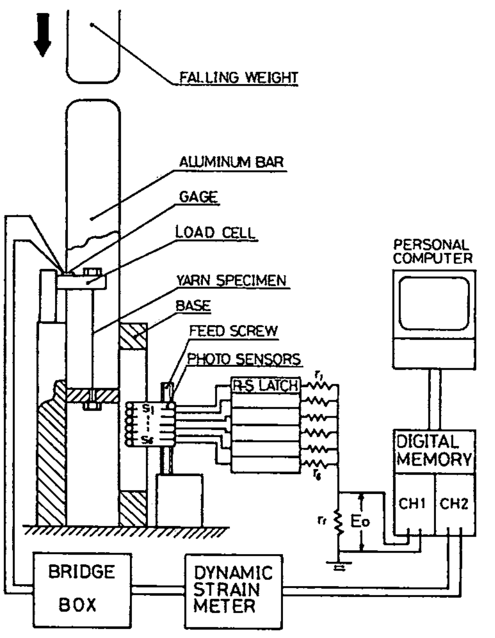

Fig.1 Schematic diagram of measurement system.

Reprinted from Proc. of Thirty-Fifth Japan Congress on Materials Research, pp.141~146 (1992)

Table 1 Strain rates

Velocity Number	①	②	③	④	⑤	⑥
Tensile Velocity (m/s)	1.6×10^{-4}	1.6×10^{-3}	1.6×10^{-2}	3.3×10^{-1}	1.67	5.33
$\dot{\varepsilon}$ (s^{-1}) (Calculated)	3.3×10^{-3}	3.3×10^{-2}	3.3×10^{-1}	6.7	33.3	108
$\dot{\varepsilon}$ (s^{-1}) (Observed)	3.3×10^{-3}	3.3×10^{-2}	3.3×10^{-1}	5.8	41.8	80

The resultant signals obtained from this strain gauge are taken into a personal computer (NEC PC9801) through the bridge box, the dynamic strain meter (KYOWA ELECTRONIC INSTRUMENTS CVD230C) and the digital memory (IWATSU DM7100). Elongation of yarn is obtained by measuring time when the lower end of the input bar crosses the photo sensors array (OMRON EE-SPZ).

Strain rates are set up six kinds as Table 1. The gauge length of each specimen is 50 mm. At low strain rates (velocity number① ~③), the input bar is pushed down by Instron-type testing machine (TOYO MEASURING INSTRUMENTS TENSILON UTM III). At high strain rates (velocity number④ ~⑥), the input bar is impacted by falling weight through the guide. Yarn specimens used in this investigation are six kinds of polyester multi-filament yarn. Their properties are shown in Table 2 and their static stress-strain curves at strain rates of 3.3×10^{-3} s^{-1} are shown in Fig.2. Yarn a, b, c differ in drawing temperature and yarn d, e, f differ in spinning speed. Experiments are performed under 20 °C and 65 %RH. after leaving the specimens in this condition more than 12 h.

3. THEORY

Equation considering strain rate dependency is as follows [2].

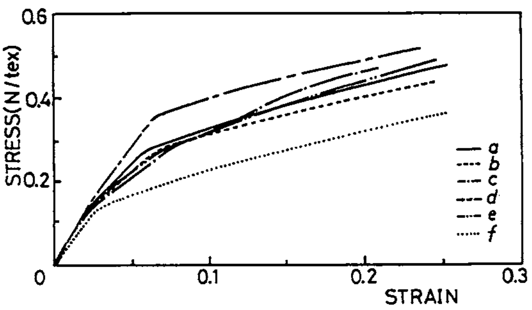

Fig.2 Static stress-strain curves of six kinds of polyester yarns investigated in this experiment at $\dot{\varepsilon} = 3.3\times10^{-3}$ s^{-1}.

Table 2 Properties of original yarns

Specimen	a	b	c	d	e	f
Filament Counts	72	72	72	36	36	36
Wet Shrinkage (%)	8.0	3.9	1.5	6.6	7.6	2.1
Crystallinity (%)	14	23	32	25	27	35
Orientation Factor(%)	90.8	92.8	93.2	86.1	90.1	94.6

$$\dot{\varepsilon} = \frac{\dot{\sigma}}{E} + \frac{\sigma - g[*]}{E\cdot K[*]} \qquad (1)$$

where σ is stress expressed in the force per unit linear density and ε is strain, the dot denotes differentiation with respect to time, the bracket [•] means the function of the argument •, g[•] is an equilibrium stress-strain at strain rate of $\dot{\varepsilon} = 0$, E is the instantaneous elastic modulus and K[•] is a material constant related to the viscous resistance. σ - g[•], the deviation of the current stress from the equilibrium stress, is called an over-stress[1]. In this investigation, the functional forms of g[•] and K[•] are empirically determined as follows [7].

$$g[\varepsilon, \theta] = g[\varepsilon, 293]\{1 + J(\theta - 293)\} \qquad (2)$$

$$E[\theta] = E[293]\{1 + J(\theta - 293)\} \qquad (3)$$

$$K = K_0 \exp\{K_1[\varepsilon](\sigma - g[\varepsilon])\} \qquad (4)$$

$$K_1 = P_0 + P_1/\dot{\varepsilon} \qquad (5)$$

Where θ is the absolute temperature and material constants E[293], J, P_0 and P_1 for each yarn are tabulated in Table 3. K_0 is 86,400 s^{-1} because above mentioned constants are determined from the 24 h stress relaxation tests[2]. g[ε, 293] is determined as a series of numerical data with 0.0005 strain intervals for each yarn from the interpolation of the 24 h relaxation tests.

Table 3 Material constants for each yarn specimen

Specimen	a	b	c	d	e	f
P_0(tex/N)	52.6	39.6	60.1	52.7	61.0	89.5
P_1(tex/N)	2.49	3.38	1.50	1.80	1.72	1.18
E (N/tex)	6.91	6.92	5.63	7.78	6.41	7.06
J	0.008	0.008	0.004	0.005	0.0055	0.003

θ', temperature rise in yarn during extension, is estimated as follows [7].

$$\theta'(\varepsilon_1) = \frac{\int_0^{\varepsilon_1} \gamma(\varepsilon)\cdot\beta(\varepsilon)\,d\varepsilon}{\beta(\varepsilon_1)} \tag{6}$$

$$\gamma(\varepsilon) = \frac{\frac{s}{\rho} - \left[\frac{\partial u}{\partial \varepsilon}\right]_T}{c_v} \tag{7}$$

$$\beta(\varepsilon) = \exp\left[\int_0^{\varepsilon} \beta'(\xi)\,d\xi\right] \tag{8}$$

$$\beta'(\varepsilon) = \frac{2h}{c_v\cdot R_0\cdot \rho\cdot \dot{\varepsilon}} \tag{9}$$

Where ρ is the density of the yarn, c_v is the thermal capacity of the yarn at constant volume and R_0 is the yarn radius. The values of ρ = 1380 kg/m^3, c_v = 1.34×10^3 J/(kg•K) [8] and R_0 = 4.38×10^{-5} m are used in this investigation. h is the heat transfer coefficient and is assumed as a constant value h = 38.5 J/(m$^2\cdot$K$\cdot$s) [8]. s is stress expressed in the force per unit cross sectional area. Only elastic energy is to be considered as internal energy u so

$$\left[\frac{\partial u}{\partial \varepsilon}\right]_T = \frac{s}{E'\cdot\rho}\cdot\frac{\partial s}{\partial \varepsilon} \tag{10}$$

where E' is the initial slope of s - ε curve.

4. EXPERIMENTAL RESULTS AND DISCUSSION

In order to obtain the effect of softening with temperature rise in filaments, tensile tests under various environmental temperature were performed at the strain rate of 3.3×10^{-3} s^{-1} using the Instron-type testing machine (ORIENTEC TENSILON RTM III) combined with the thermal bath (YASHIMA WORKS TCF-R2). Results for yarn e are shown in Fig.3 for example. Solid lines are experimental data and dotted lines are calculated from Eqs.(2) and (3). Other yarns also have shown similar tendency. The value of constants J for all yarns tested, that express the effect of softening with temperature rise, are listed in Table 3 above mentioned.

Numerical results of temperature rise in yarn during extension estimated by means of Eq.(6) are shown in Fig.4 for yarn e. Numbers in circles indicate the velocity number in Table 1 respectively. The curve for① shows scarcely temperature rise. In②, yarn extension proceeds almost isothermally and temperature rise is less than 10 °C at 20 % strain. On the contrary, temperature rise in③ is more than 10 °C at 10 % strain. Furthermore, extension proceeds almost adiabatically at higher strain rate as shown in④,⑤ and⑥. In these cases, calculated temperature rises are about 15 °C at 10 % strain and about 45 °C at 20 % strain. Results for other yarns have been almost same as Fig.4 except for yarn f that has shown some smaller temperature rise because of smaller stress at the same strain as shown in Fig.2.

Stress-strain curves of various strain rates for each yarn obtained from tensile experiments are shown in Fig.5 ~ Fig.10 by solid lines. Theoretical curves obtained from numerical calculation of Eq.(1) considering the effect of softening with temperature rise in filaments during extension by means of Eqs. (2) ~ (10) are also shown in the same figures by dotted lines. Both curves agree closely in any yarns and in any strain rates. Therefore predictive capability of this constitutive equation for various polyester multi-filament yarns at strain rates ranging from the order of 10^{-3} to 10^2 s^{-1} are ascertained.

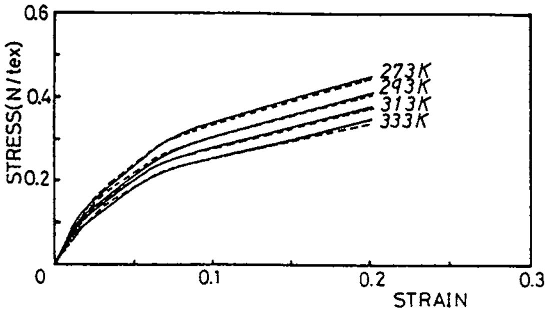

Fig.3 Stress-strain curves of yarn e at $\dot{\varepsilon}$ = 3.3×10^{-3} s^{-1} for various temperature. Solid lines are experimental data, dotted lines are calculated from Eqs. (2) and (3).

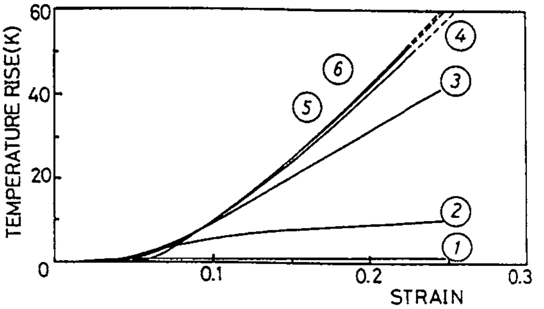

Fig.4 Estimated temperature rise during extension at various strain rates. Numbers in circles are the velocity number in Table 1.

5. CONCLUSION

The constitutive equation based on the over-stress theory had well explained the stress-strain curves of polyester multi-filament yarn at low strain rates. But the calculated stress had become larger than experimental data with increasing strain and strain rate at high strain rates. In this study, therefore, estimating the temperature rise in filaments during extension and measuring the degree of softening with temperature rise, we proposed the dynamic constitutive equation considering temperature. And this constitutive equation were compared with the stress-strain curves of six kinds of polyester multi-filament yarn which had various mechanical properties due

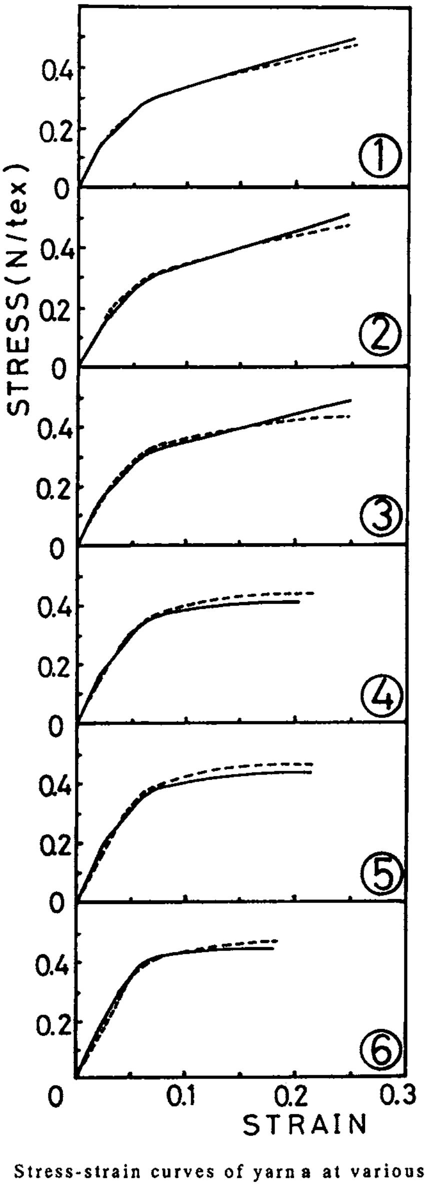

Fig.5 Stress-strain curves of yarn a at various strain rates. Solid lines are experimental data and dotted lines are calculated from Eq. (1). Numbers in circles are the velocity number in Table 1.

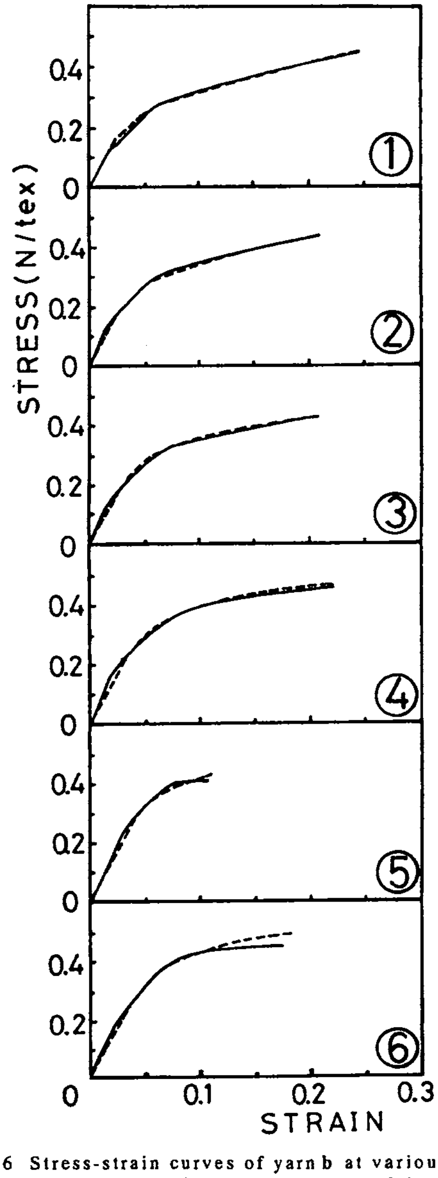

Fig.6 Stress-strain curves of yarn b at various strain rates. Solid lines are experimental data and dotted lines are calculated from Eq. (1). Numbers in circles are the velocity number in Table 1.

to differ in drawing temperature or in spinning speed at strain rates ranging from the order of 10^{-3} to 10^{2} s^{-1}. Close agreement between observed and calculated curves for all yarns proved the predictive capability of this constitutive equation for polyester multi-filament yarns.

ACKNOWLEDGEMENTS

The authors wish to thank Prof. Chatani for his helpful advice and also Mr. M.Minami, N.Hayashi, N.Matsumori and T.Murata for their experimental assistance.

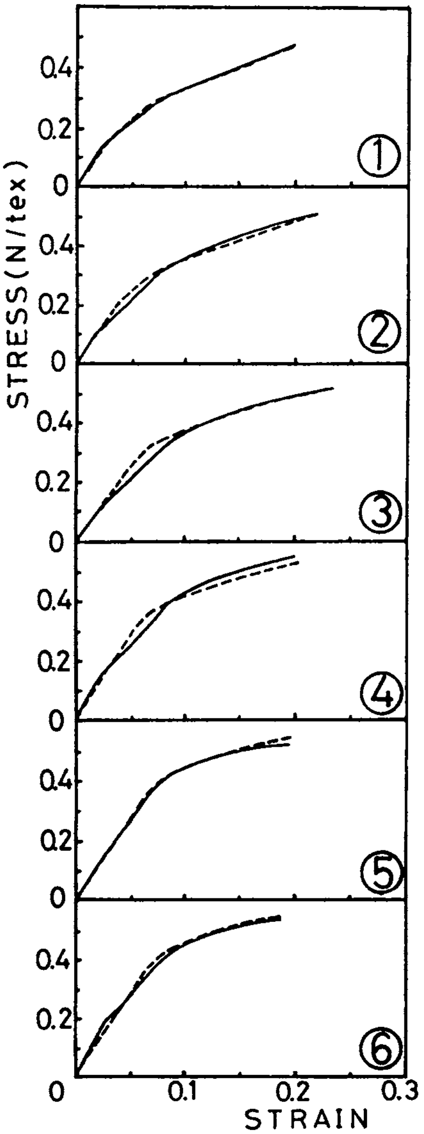

Fig.7 Stress-strain curves of yarn c at various strain rates. Solid lines are experimental data and dotted lines are calculated from Eq. (1). Numbers in circles are the velocity number in Table 1.

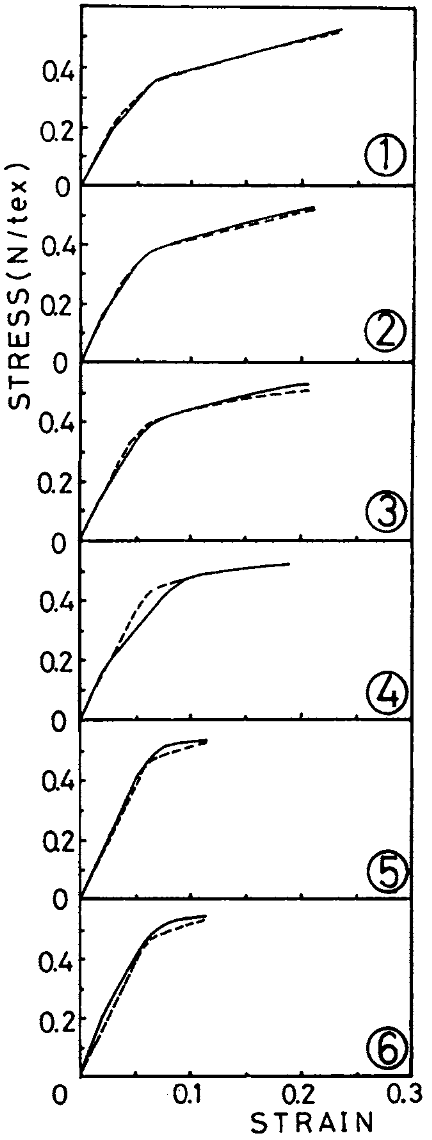

Fig.8 Stress-strain curves of yarn d at various strain rates. Solid lines are experimental data and dotted lines are calculated from Eq. (1). Numbers in circles are the velocity number in Table 1.

REFERENCES

1) M.C.Liu, E.Krempl:J. Mech. Phys. Solid, 27, 377 (1979)
2) T.Kinari, A.Hojo, S.Shintaku, N.Iwaki: Sen-i Gakkaishi, 311, 46 (1990) (In Japanese)
3) W.K.Stone, H.F.Schifer, G.Fox : Text. Res.J., 25, 520 (1955)
4) W.Itani, T.Wada, K.Asada and Y.Shimizu: Sen-i Gakkaishi, 43,24(1968)(In Japanese)
5) W.Itani, T.Wada, K.Asada and Y.Shimizu: Sen-i Gakkaishi,48,24(1968)(In Japanese)
6) I.H.Hall: J.Appl.Polymer Sci.,739,12 (1968)
7) T.Kinari, A.Hojo, S.Shintaku, N.Iwaki:J. Text. Mach. Jap., T118,44(1991) (In Japanese)
8) T.Yamamoto, S.Shintaku, T.Kinari:Sen-i Gakkaishi, 457, 44 (1989) (In Japanese)

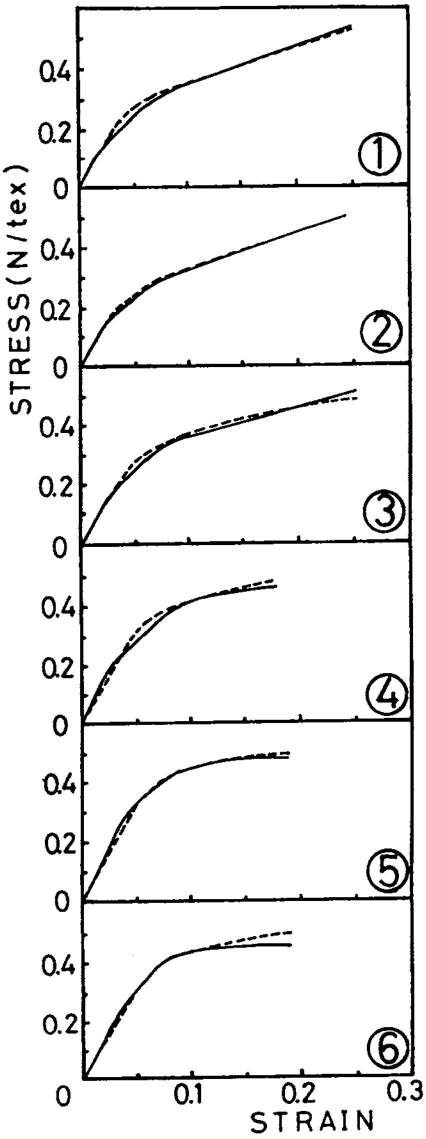

Fig.9 Stress-strain curves of yarn e at various strain rates. Solid lines are experimental data and dotted lines are calculated from Eq. (1). Numbers in circles are the velocity number in Table 1.

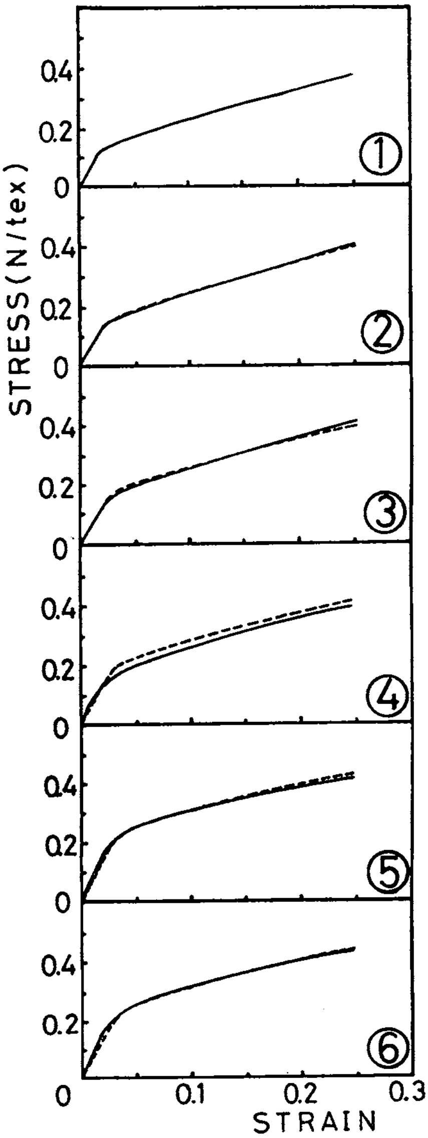

Fig.10 Stress-strain curves of yarn f at various strain rates. Solid lines are experimental data and dotted lines are calculated from Eq. (1). Numbers in circles are the velocity number in Table 1.